Multi-color fluorescence imaging based on plasmonic wavelength selection and double illumination by white light

Jong Min Choi,[1] Kyungsik Eom,[2] Seoyoung Hwang,[3] Yena Lee,[3] Sang Beom Jun,[3] Kyung Min Byun,[1,*] and Sung June Kim[2]

[1]*Department of Biomedical Engineering, Kyung Hee University, Yongin 446-701, South Korea*
[2] *School of Electrical Engineering and Computer Science, Seoul National University, Seoul 151-742, South Korea*
[3]*Department of Electronics Engineering, Ewha Womans University, Seoul 120-750, South Korea*
**kmbyun@khu.ac.kr*

Abstract: We demonstrate the proof-of-concept for developing a multi-color fluorescence imaging system based on plasmonic wavelength selection and double illumination by white light source. This technique is associated with fluorescence excitation by transmitted light via a diffraction of propagating surface plasmons. Since double illumination through both sides of isosceles triangle prism in the Kretschmann configuration enables multiple transmission beams of different wavelengths to interact with the specimen, our approach can be an alternative to conventional fluorescence detection owing to alignment stability and functional expandability. After fabricating a plasmonic wavelength splitter and integrating it with microscopic imaging system, we successfully confirm the performance by visualizing in vitro neuron cells labeled with green and red fluorescence dyes. The suggested method has a potential that it could be combined with plasmonic biosensor scheme to realize a multi-functional platform which allows imaging and sensing of biological samples at the same time.

OCIS codes: (170.0110) Imaging systems; (180.2520) Fluorescence microscopy; (240.6680) Surface plasmons; (050.1950) Diffraction gratings.

References and links

1. J. W. Lichtman and J.-A. Conchello, "Fluorescence microscopy," Nat. Methods **2**(12), 910–919 (2005).
2. P. T. Tran and F. Chang, "Transmitted light fluorescence microscopy revisited," Biol. Bull. **201**(2), 235–236 (2001).
3. S. E. Raza, A. Humayun, S. Abouna, T. W. Nattkemper, D. B. A. Epstein, M. Khan, and N. M. Rajpoot, "RAMTaB: Robust alignment of multi-tag bioimages," PLoS ONE **7**(2), e30894 (2012).
4. P. Matula, M. Kozubek, F. Staier, and M. Hausmann, "Precise 3D image alignment in micro-axial tomography," J. Microsc. **209**(2), 126–142 (2003).
5. J.-C. Song, W. K. Jung, N.-H. Kim, and K. M. Byun, "Plasmonic wavelength splitter based on a large-area dielectric grating and white light illumination," Opt. Lett. **37**(18), 3915–3917 (2012).
6. W. K. Jung, N.-H. Kim, and K. M. Byun, "Development of a large-area plasmonic sensor substrate with dielectric subwavelength gratings using nanoimprint lithography," J. Biomed. Nanotechnol. **9**(4), 685–688 (2013).
7. M. G. Moharam, D. A. Pommet, E. B. Grann, and T. K. Gaylord, "Stable implementation of the rigorous coupled-wave analysis for surface-relief gratings: enhanced transmittance matrix approach," J. Opt. Soc. Am. A **12**(5), 1077–1086 (1995).
8. Y. Kanamori, K. Hane, H. Sai, and H. Yugami, "100 nm period silicon antireflection structures fabricated using a porous alumina membrane mask," Appl. Phys. Lett. **78**(2), 142 (2001).
9. Q. Cao and P. Lalanne, "Negative role of surface plasmons in the transmission of metallic gratings with very narrow slits," Phys. Rev. Lett. **88**(5), 057403 (2002).
10. K. M. Byun, S. J. Yoon, D. Kim, and S. J. Kim, "Experimental study of sensitivity enhancement in surface plasmon resonance biosensors by use of periodic metallic nanowires," Opt. Lett. **32**(13), 1902–1904 (2007).
11. L. Li and C. W. Haggans, "Convergence of the coupled-wave method for metallic lamellar diffraction gratings," J. Opt. Soc. Am. A **10**(6), 1184–1189 (1993).
12. S. H. Jeong, S. B. Jun, J. K. Song, and S. J. Kim, "Activity-dependent neuronal cell migration induced by electrical stimulation," Med. Biol. Eng. Comput. **47**(1), 93–99 (2009).

#204017 - $15.00 USD Received 2 Jan 2014; revised 23 Feb 2014; accepted 24 Feb 2014; published 6 Mar 2014

13. T. L. Fletcher, P. Cameron, P. De Camilli, and G. Banker, "The distribution of synapsin I and synaptophysin in hippocampal neurons developing in culture," J. Neurosci. **11**(6), 1617–1626 (1991).
14. S. H. Choi, S. J. Kim, and K. M. Byun, "Design study for transmission improvement of resonant surface plasmons using dielectric diffraction gratings," Appl. Opt. **48**(15), 2924–2931 (2009).
15. K. M. Byun, S. J. Kim, and D. Kim, "Grating-coupled transmission-type surface plasmon resonance sensors based on dielectric and metallic gratings," Appl. Opt. **46**(23), 5703–5708 (2007).

1. Introduction

Fluorescence microscopy has been successful in a variety of biological applications due to its remarkable sensitivity, high specificity, and possibility of live cell imaging [1]. In principle, the optical path of fluorescence signal is relatively simple: white light passing through an excitation filter is reflected by dichroic mirror into the objective lens to illuminate the sample and then the excited sample emits fluorescent light, which is re-collected by the objective lens and passed through the emission filter to camera [2]. However, despite such advantages, there are several drawbacks inherent in fluorescence microscopy: a) mechanical switching of filter cubes to see different color fluorescence can cause misalignment of images; b) high-priced multi-passband filter cubes can eliminate the misalignment problem, but may attenuate the emission light; and c) fluorescent light source cannot be used in combination with transmitted light techniques such as phase or differential interference contrast microscopy [3,4].

We recently demonstrated an optical process by which the wavelengths of transmitted light can be divided selectively by changing a resonance angle of surface plasmons in the presence of dielectric gratings [5]. For transverse magnetic (TM)-polarized light, if an incidence beam satisfies the condition of surface plasmon resonance (SPR), the electromagnetic field is strongly enhanced and confined in the vicinity of the metal surface as a non-radiative evanescent field. When white light is incident to a gold substrate with a dielectric grating, the propagating surface plasmons are transmitted into the air via diffraction by a large-area grating pattern fabricated by nanoimprint lithography [6]. As the transmitted beam of a certain wavelength can be selected by changing an illumination angle of the white light, plasmonic wavelength splitter is feasible for transmission-type fluorescence imaging to overcome the limitations of conventional fluorescence microscopy described above.

For the proposed strategy, the specimen is intended to be illuminated by diffraction light obtained from the dielectric grating and the fluorescent emission is captured by objective lens. This approach eliminates the need of switching excitation filters and dichroic mirrors. However, in the case of single beam excitation with rotation stage and mirror for adjusting an incidence angle, it is often difficult to prevent the optical path from being slightly deviated. Hence, we adopt a double illumination scheme combined with different incident beams passing through both sides of isosceles triangle prism, which is advantageous in terms of alignment stability and system robustness.

In this study, we aim to demonstrate an alternative imaging technique that enables a multi-color fluorescent excitation by two independent diffractions of surface plasmons in a controlled fashion. The plasmonic wavelength splitter examined here is simpler than conventional filter cubes containing excitation filters and dichroic mirrors that have been generally used for fluorescence imaging. Also, color selectivity of the proposed platform can be easily tuned by using the resonant wavelength dependence of surface plasmons. It is expected that our suggestion could be an attractive candidate for advanced analytical tool for monitoring the activities of biological samples at the substrate surface as well as imaging their structures selectively, when it is combined with the principle of SPR biosensing.

2. Materials and methods

2.1. Numerical model

Schematic of plasmonic wavelength splitter is shown in Fig. 1. The numerical model presents that a thin gold film with a thickness of 45 nm is coated on a SF10 glass via an attachment of 5-nm thick titanium adhesion layer. One dimensional rectangular SiO_2 grating with a period of Λ, a width of w, and a thickness of d is regularly patterned on the gold/SF10 glass

#204017 - $15.00 USD Received 2 Jan 2014; revised 23 Feb 2014; accepted 24 Feb 2014; published 6 Mar 2014

substrate, while TM-polarized white light illuminates the substrate at an incidence angle of θ. When the white light is incident with a given angle satisfying the momentum matching condition between surface plasmons and incident photons, only TM-polarization field is completely transferred to surface plasmon waves and is then converted into a radiative light field by dielectric gratings. On the other hand, transverse electric (TE) field cannot couple with surface plasmons and thus no transmission mode is generated. This condition is expressed as

$$k_q = k_{\mathrm{SPR}} - qK = k_0\sqrt{\varepsilon_p}\sin\theta_{\mathrm{SPR}} - q\frac{2\pi}{\Lambda}. \tag{1}$$

where k_q, k_{SPR}, and k_0 are the wave vectors of the transmitted light with q-th diffraction order, the plasmon waves and the incident light, respectively. K is the grating vector and ε_p and θ_{SPR} are the dielectric function of a glass substrate and the incidence angle at resonance. The angle of q-th diffracted beam is given by

$$\theta_q^T = \sin^{-1}\left(k_q / k_0\right). \tag{2}$$

For fixed wavelength, the number of transmitted beams is determined by the diffraction angle that satisfies the above relation. In this study, a limited range of grating period and thickness is considered to suppress the high-order diffraction beams, so that only the low diffraction orders can radiate into the air.

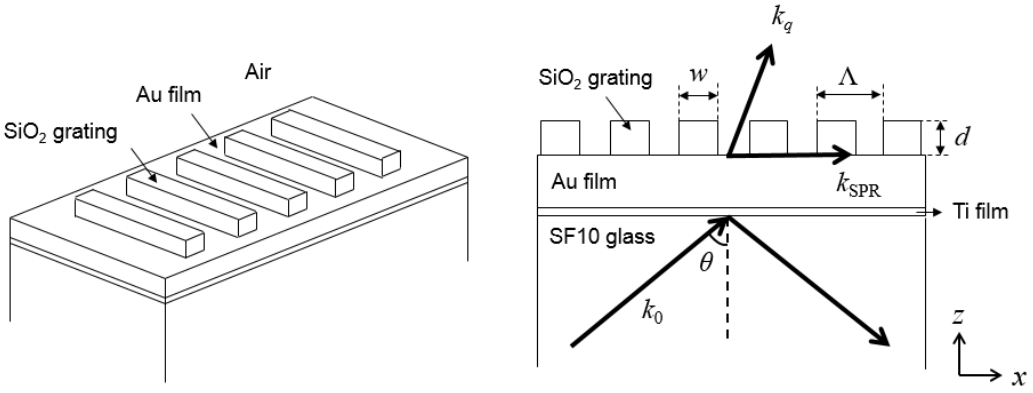

Fig. 1. Perspective image of the plasmonic wavelength splitter and its cross-sectional view. Dielectric SiO_2 gratings are regularly patterned on a 45-nm thick planar gold film. The grating structure of a rectangular profile has a period of Λ, a width of w, and a thickness of d. When a TM-polarized white light is incident through a gold/titanium/SF10 substrate with an angle of θ, the resonant surface plasmon waves radiate into the air environment by diffraction gratings and the color of transmitted light is determined by the wavelength-dependence of SPR. As the high-order diffraction beams are suppressed for given grating period and thickness, only the first-order diffraction is considered as a transmission mode.

In order to investigate the relationship between the incident angle of white light and the wavelength of diffracted beam, numerical simulations based on rigorous coupled-wave analysis (RCWA) method are employed [7]. RCWA has been successfully used to explain the experimental results of various grating-mediated structures [8,9]. Our RCWA routine was also proved to corroborate the experiments of earlier SPR studies based on periodic dielectric or metallic nanostructures [10]. Note that, since the field varies more rapidly in short distances of a grating with a size smaller than a wavelength λ, more space-harmonic orders are required to achieve the convergence and to improve the accuracy in calculations. For the

#204017 - $15.00 USD Received 2 Jan 2014; revised 23 Feb 2014; accepted 24 Feb 2014; published 6 Mar 2014

calculation presented in this study, 30 spatial harmonics have been considered and convergence in RCWA computation was successfully achieved [11].

2.2. Sample preparation

In fabrication, a 45-nm thick gold film is sputtered onto an SF10 glass after an evaporation of a 5-nm thick titanium adhesion layer. Ar gas (40 sccm) is used under a 4 mTorr chamber pressure at 250W RF power for gold and at 300W DC power for titanium. SiO_2 layer with a thickness of 100 nm is then deposited on the gold film via electron beam evaporation at room temperature. Before pressing the stamp which contains a designed grating structure into the imprint resist (NIP-SC58LV100, Chem Optics, Korea), an additional film of polymethyl methacrylate (PMMA) is spin-coated, so that this PMMA film acts as a cushioning layer that protects the fragile nanoscale features on the stamp surface. After a 200-nm thick PMMA layer is obtained at a speed of 1,000 rpm for 60 sec, it is baked at 170°C for 300 sec.

During the nanoimprint lithography (NIL) patterning process, a large-area stamp with high-feature density creates a deep thickness contrast of about 150 nm in the imprint resist. After the stamp is peeled off from the substrate, PMMA and SiO_2 layers are etched by O_2 plasma ashing for 120 sec and by anisotropic dry etching with a 9:1 SF_6-O_2 mixture for 60 sec, respectively. Finally, the residual polymers are removed by acetic acid and distilled water.

2.3. Neuron cell culture

Primary hippocampal neurons are obtained by referring to the works by Jeong et al. [12]. Whole brains are isolated from fetuses of embryonic day 17 Sprague-Dawley rats (Samtako, Korea) and are placed in sterile buffered saline solution (BSS). Hippocampi are dissected from the separated cerebral hemispheres, placed in ice-cold BSS and incubated in 0.25% trypsin (Sigma Aldrich, USA) for 15 min at 37þC. Digested hippocampi are dissociated and seeded at the density of 600 cells/mm^2. Serum-free neurobasal media (21103, Gibco®, USA) supplemented with 2% B27 (17504-044, Gibco®, USA) and 1% Glutamax (35050, Gibco®, USA) are used as a culture media. Cultured cells are maintained at 37°C in 5% CO_2 and 95% air humidified atmosphere before fluorescence experiments.

For staining, neuron cells are fixed with 4% paraformaldehyde (37°C for 15 min); permeablized with 1% Triton X-100 in HBHS for 15 min at room temperature; and incubated in 6% bovine serum albumin for 30 min at room temperature to block nonspecific binding. Samples are then exposed to a mixture of rabbit polyclonal anti-MAP2 (Sigma, 1:500) and mouse monoclonal anti-synaptophysin (Sigma, 1:200) for 1 h at 37°C. After washing, samples are additionally incubated with secondary antibodies, Texas Red goat anti-rabbit (Molecular Probes, Eugene OR, 1:200) and Alexa Fluor 488 goat anti-mouse (Molecular Probes, 1:200) for 1 h at 37°C. Positive MAP-2 labeling identifies neuronal cell bodies and dendrites. Distribution of positive labeling for synaptophysin, a presynaptic protein, is used to identify potential synaptic sites [13].

2.4. Fluorescence imaging setup

As soon as the fabricated sample is loaded onto an isosceles triangle prism via index matching oil, fluorescence studies on the target neurons are performed by the imaging setup presented in Fig. 2. Divergent light from the white source (#66995 QTH, Oriel instruments) is collimated by collimation lens and light guide (Liquid light guide, Oriel instruments). Then, a beam-splitter divides the polarized white light into two beams before entering a prism in the standard Kretschmann configuration and each one is incident to the substrate with a fixed angle determined by a mirror. Together with allowing light to couple into the cells, a 20 × objective lens (NA 0.4, Olympus) collects fluorescence emission which passed through the labeled neurons. Two electromechanical shutters pass a light by turns to permit a single exposure for fluorescence excitation on the specimen. The fluorescence emission is spectrally filtered by an emission filter (520/10 nm and 620/10 nm, Edmund optics) to reduce the effect of any scattered and transmitted light and is finally focused on a CCD camera (QICAM 1394,

#204017 - $15.00 USD Received 2 Jan 2014; revised 23 Feb 2014; accepted 24 Feb 2014; published 6 Mar 2014

QImaging). The field of view is 1.1 × 1.1 mm^2 and this value is determined by the magnification of objective lens and the sensor size of CCD camera.

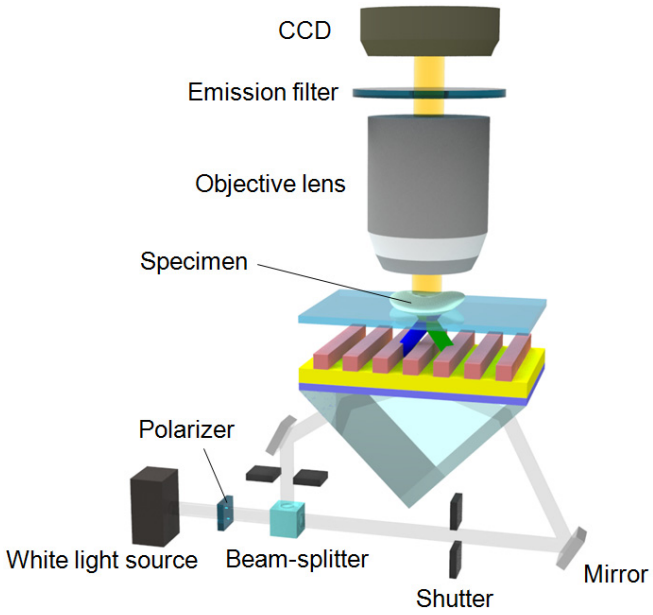

Fig. 2. Experimental setup of multi-color fluorescence imaging system combined with a plasmonic wavelength splitter. Optical elements for double illumination include linear polarizer, 50:50 beam-splitter, mirrors, and electromechanical shutters. The image detection part consists of objective lens, emission filter, and CCD camera. Diameter of the transmitted beam is equal to 10 mm.

3. Results and discussion

First of all, in order to improve a color selectivity of the plasmonic wavelength splitter, the thickness of SiO_2 grating must be optimized. The period and width of SiO_2 grating are fixed at Λ = 400 nm and w = 200 nm because a significant reduction of diffraction efficiency was found at the grating period of Λ = 450 ~500 nm and $\Lambda \leq$ 300 nm from our previous study [14]. Figure 3(a) shows a relation between incidence wavelength and its corresponding resonance angle based on RCWA computation. Four different cases are chosen based on an assumption that a controllable thickness resolution of SiO_2 grating is estimated to be 50 nm in our fabrication conditions. We find that resonance angle contrast between red (λ = 600 nm) and blue (λ = 400 nm) is decreased with an increasing grating thickness. The incidence angles for the two colors are, respectively, 41.8° and 58.0° for d = 50 nm, 46.2° and 58.9° for d = 100 nm, and 48.5° and 59.1° for d = 150 nm, indicating that the SiO_2 grating of d = 50 nm can provide the highest color selectivity to separate colors for fluorescence excitation.

Contrary to a decreasing resonance angle contrast, diffraction efficiency at λ = 600 nm increases and reaches over 20% with an increment of grating thickness as shown in Fig. 3(b). Such a growing trend is degraded when d > 150 nm and then finally saturates. No further increase of diffraction efficiency can be explained by a limited penetration depth of surface plasmon waves [15]. It has been well known that the field intensity of surface plasmon decays rapidly when one moves further away from the metal surface. As a result, when taking a controllable resolution of grating thickness, resonance angle contrast, and diffraction efficiency into consideration, the optimized grating thickness is determined to be d = 100 nm.

#204017 - $15.00 USD Received 2 Jan 2014; revised 23 Feb 2014; accepted 24 Feb 2014; published 6 Mar 2014

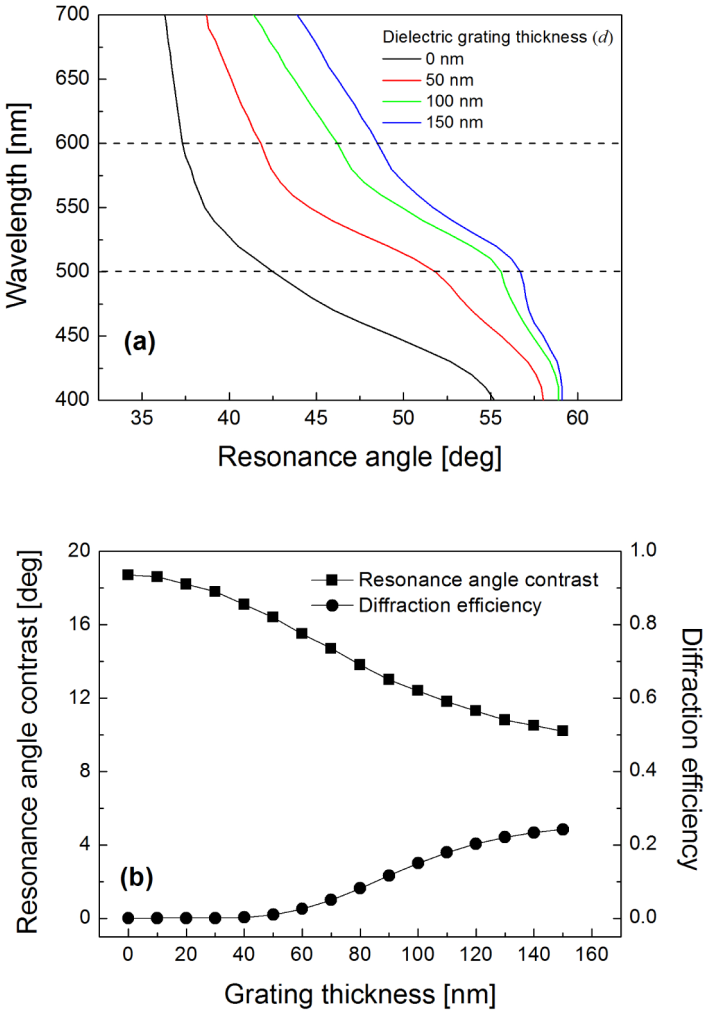

Fig. 3. (a) Calculated relationship between incidence wavelength and resonance angle. (b) Resonance angle contrast and diffraction efficiency at λ = 600 nm, when a thickness of SiO_2 grating varies from 0 to 150 nm in a step of 10 nm. With an increasing thickness, diffraction efficiency gradually grows over 20%, while SPR angle contrast between red and blue colors is decreased.

Large-area pattern of dielectric gratings can be successfully realized by using NIL-based fabrication process described in the section *2.2*. Top and cross-sectional images of the samples are presented in Figs. 4(a) and 4(b). The period, width, and thickness of SiO_2 gratings are 400, 200, and 100 nm. Total effective area of the patterned dielectric gratings is approximately 5 × 5 mm^2. To demonstrate a color selectivity of the fabricated plasmonic wavelength splitter, we adjust a resonance angle of collimated white light and find that the radiation mode is successfully decomposed into different colors. When a 250 W white light is incident on the SPR samples, averaged diffraction beam powers are measured to be 3.2 mW for red, 2.7 mW for yellow, 2.0 mW for green, and 0.5 mW for blue, which matches well the trend of spectral curves obtained by a wide range spectrometer (BLK-CXR-SR, StellarNet Inc., USA) in Fig. 4(c). A weak transmission intensity for blue color is attributed to the fact that the proposed wavelength splitter provides a relatively low diffraction efficiency at shorter wavelengths of visible light. While the detailed results are not shown here, we found that the diffraction intensity is reduced to a few percent of the input, especially in the wavelengths of

#204017 - $15.00 USD Received 2 Jan 2014; revised 23 Feb 2014; accepted 24 Feb 2014; published 6 Mar 2014

blue color. Moreover, as the unpolarized white light suffers an initial 50% loss by TM-polarizer, use of high power source is demanded for applications where high excitation intensities are necessary. However, we can reduce the input power and improve the proposed scheme by utilizing an advanced CCD camera with a higher sensitivity and objective lens with a higher NA. Figure 4(d) shows a comparison of experimental data in Fig. 4(c) with numerical results for d = 100 nm in Fig. 3(a). Incidence angle, denoted by a filled square, and full-width at half-maximum (FWHM) of transmission spectrum, denoted by an error bar, are 57° and 48 nm for blue of λ = 476 nm, 55° and 44 nm for green of λ = 520 nm, 49° and 46 nm for yellow of λ = 580 nm, and 46° and 46 nm for red of λ = 609 nm, respectively. When d = 100 nm, it is confirmed that the experimental results are well consistent with the RCWA simulations. Slight contrast between numerical and experimental data is attributable to defects and errors in the fabrication processes.

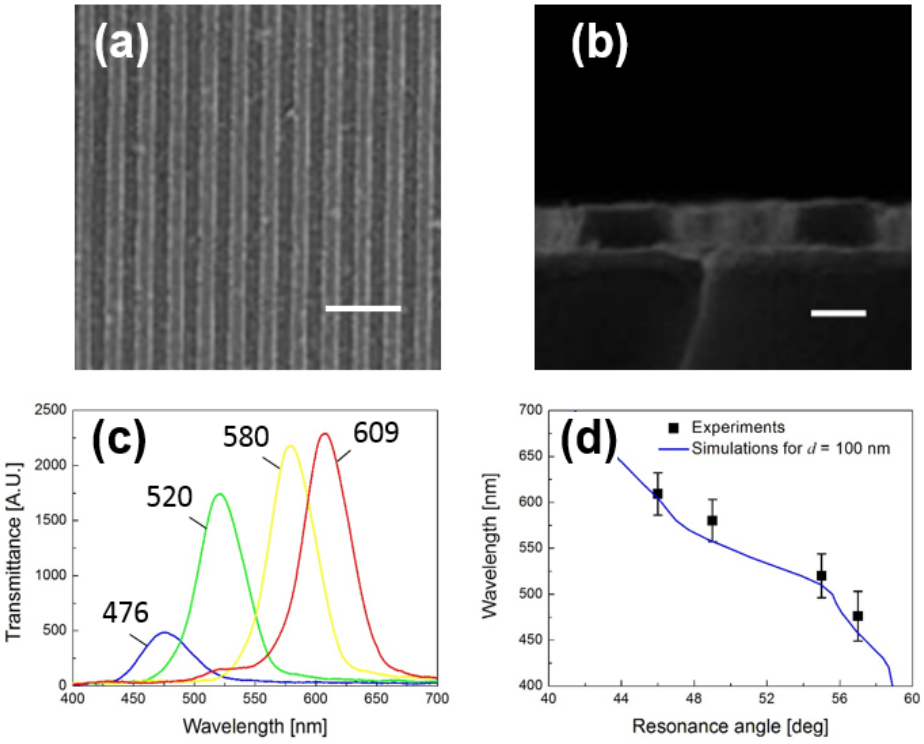

Fig. 4. (a) Top-view and (b) cross-sectional scanning electron microscope images of a large-area grating pattern of the fabricated plasmonic wavelength splitter. Scale bar is 1 μm for (a) and 100 nm for (b). (c) Measured transmission spectra when an incidence angle of white light is varied. Illumination angle is 57° for blue, 55° for green, 49° for yellow, and 46° for red, respectively. (d) Comparison between experimental data and RCWA simulations for d = 100 nm. Error bars denote the FWHM values of transmission curves in Fig. 4(c).

Due to such transmission unevenness, particularly for the band of blue color, we choose labels in green (Alexa Fluor 488) and red (Texas Red) for fluorescence imaging experiments. When a double illumination with different incidence angles of white light is applied to the specimen as shown in Fig. 2, two incidence conditions can be manipulated to induce a multi-color fluorescence excitation. To demonstrate this, experiments using a liquid solution containing green and red fluorescence dyes are performed by comparing the average fluorescence intensity for TE and TM polarizations. Figure 5 presents the measured fluorescence intensity profiles under the double illumination condition. When TM-polarized white light is incident with angles corresponding to the excitation wavelengths, diffracted surface plasmons by surface-relief dielectric gratings generate an emission by the

#204017 - $15.00 USD Received 2 Jan 2014; revised 23 Feb 2014; accepted 24 Feb 2014; published 6 Mar 2014

fluorescence dyes, while no fluorescence signal is found for TE polarization. We confirm that the fluorescence emission is highly associated with an excitation of surface plasmons and as a result, wavelength selection by plasmonic wavelength splitter can replace the function of filter cubes containing excitation filters and dichroic mirrors used in a conventional fluorescence imaging system. In addition, the average intensity values of the obtained signals, in 4 separate measurements, are: 262 ± 21 of signal / 9.2 ± 1.2 of background for green and 248 ± 25 of signal / 23.0 ± 3.2 of background for red fluorescence. Since our fluorescence scheme produces a slightly high background noise with a signal to noise ratio from 5 to 10 percent, the scattered light components in excitation should be reduced to as low a level as possible to obtain a good image quality.

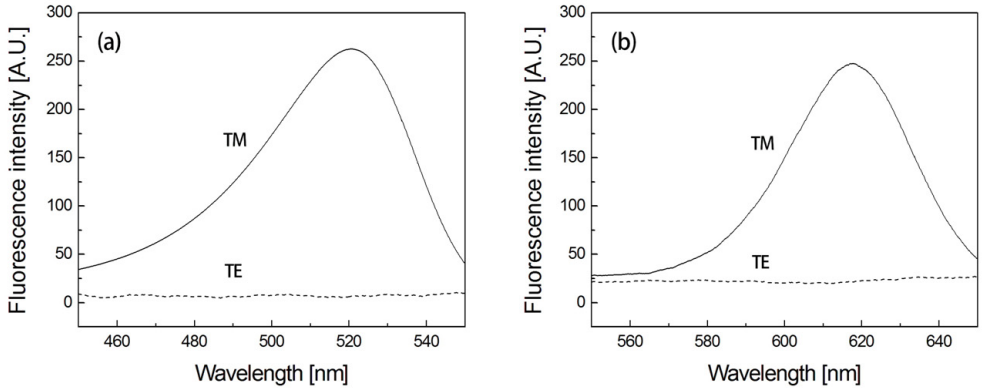

Fig. 5. Fluorescence intensity spectra obtained for (a) Alexa Fluor 488 and (b) Texas Red, depending on the polarization of white light. For TM-polarization, transmission light generated excites the given fluorescence sample effectively, while TE-polarized beam does not produce any fluorescence signal due to no excitation of surface plasmons.

Finally, fluorescence images of in vitro neuron cells are acquired on the suggested platform. A typical bright field image of the cultured neuron cells is shown in Fig. 6(a), where the signal is simply generated by absorption as light passes through the sample. Bright field images of biological samples tend to have a morphological outline, because most cells are not strongly light-absorbing. On the other hand, using green and red fluorescence dyes, specific targets are selectively shown against dark background in Figs. 6(b) and 6(c). In our experiments, green fluorescence is conjugated with the regions containing presynaptic proteins, while red fluorescence is observed in the cell body and dendrites. As distribution of positive labeling for synaptophysin, a presynaptic protein, is used to identify potential synaptic sites, the obtained results present that presynaptic sites are widely distributed in the cultured neural networks. While the fluorescence emission is spectrally filtered by an emission filter to reduce the effect of any scattered and transmitted light, the captured images may contain a small amount of out-of-focus light from the given structure and thus reduce the sharpness and contrast of the structure. This problem can be effectively defeated in the confocal microscope by stopping down the pinhole aperture in order to reject the maximum amount of out-of-focus light and reduce flare.

It should be also emphasized that, in our multi-color fluorescence imaging setup, wavelength selection does not require any change of filter cubes except for manual switching of emission filter in front of CCD camera. This may provide better optical alignment and system robustness. Further, it is expected that our transmission-type imaging scheme could be combined with advanced techniques such as phase or differential interference contrast microscopy, while no related experiment has not been performed here.

#204017 - $15.00 USD Received 2 Jan 2014; revised 23 Feb 2014; accepted 24 Feb 2014; published 6 Mar 2014

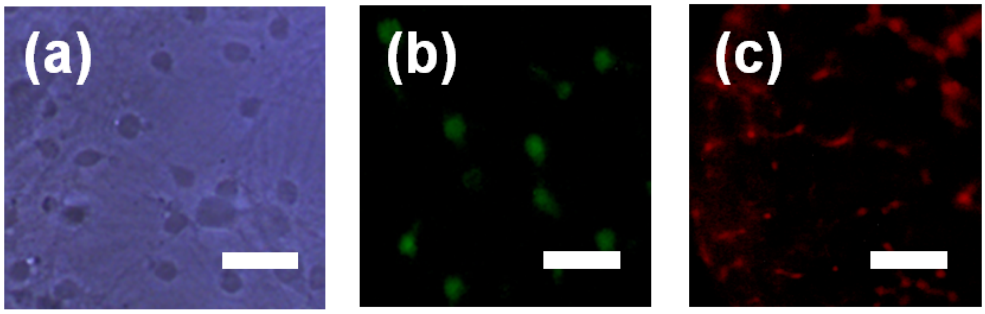

Fig. 6. Microscope images of neuron cells fixed on a glass substrate. (a) Bright field image. (b) Distribution of the presynaptic protein synaptophysin labeled by Alexa Fluor 488. (c) Labeling of dendrites and cell bodies using Texas Red with MAP-2 primary antibodies. Scale bar = 50 μm.

4. Conclusion

In this study, we demonstrate the proof-of-concept for multi-color fluorescence imaging through a combination of plasmonic wavelength splitter and double illumination by white light. A large-area SiO_2 grating of Λ = 400 nm and d = 100 nm is successfully realized using nanoimprint lithography and shows a fairly good performance in terms of color selectivity. While the diffraction efficiency for shorter wavelengths needs be improved, green and red fluorescence signals are efficiently produced only for TM polarization, which implies that fluorescence emission is accompanied by an excitation of surface plasmons. Moreover, although very preliminary, we confirm the feasibility of the proposed scheme by visualizing biological samples from fluorescence experiments for cultured neuron cells and therefore expect its potential for integration with SPR biosensing scheme to realize a multi-functional platform which allows imaging and sensing of biological samples at the same time.

Acknowledgments

We acknowledge the support of Korea Science and Engineering Foundation (KOSEF) grant funded by the Korean government (MEST) (2011-0029485). This work was also supported by NSF-2013R1A1A1A05011990 and by MSIP as Global Frontier Project (CISS-2013072261). Sung June Kim acknowledges the support by the Brain Korea 21 Plus Project in the Department of Electrical and Computer Engineering, Seoul National University in 2014.